Journal of Fundamental and Applied Research **Vol. 5**, Issue 4 (2025) **20250027**

Received: 14 November 2025 / Accepted: 22 December 2025
Published online: 22 December 2025
© 2025 The Author(s)

Charged particles orbiting magnetized Schwarzschild black holes Kalb Ramond gravity

Mukhabbat Kurbanova[1,2,*] and Nuriddin Kurbonov[3,4,†]

[1]*Institute of Fundamental and Applied Research, National Research University TIIAME, Kori Niyoziy 39, Tashkent 100000, Uzbekistan*
[2]*American University of Technology, Beshyogoch street 1, Tashkent 100060, Uzbekistan*
[3]*Institute for Advanced Studies, New Uzbekistan University, Movarounnahr str. 1, Tashkent 100000, Uzbekistan*
[4]*Tashkent State Technical University, Tashkent 100095, Uzbekistan*

Abstract. In this study, we investigate the motion of electrically charged particles orbiting a magnetized Schwarzschild black hole(BH) within the framework of Kalb–Ramond(KR) gravity. Assuming a uniform external magnetic field, we analyze the effective potential, circular orbits, and the properties of the innermost stable circular orbit(ISCO). We show that both the magnetic field coupling and the KR parameter significantly modify orbital dynamics and stability. Negative magnetic coupling enhances the effective potential barrier and stabilizes circular motion, while positive coupling weakens confinement. The KR parameter further alters this behavior, with negative values allowing higher angular momentum at lower energies and positive values acting in the opposite direction. We find that increasing the magnetic field strength shifts the ISCO radius inward, increases angular momentum, and lowers the ISCO energy, whereas negative KR corrections shift the ISCO outward and reduce its energy. These results demonstrate that KR gravity introduces nontrivial modifications to charged particle motion in magnetized BH spacetimes.

Key words: black hole, Schwarzschild black hole, Kalb-Ramond gravity, innermost stable circular orbit.

I. INTRODUCTION

Black holes, as solutions to Einstein's equations in general relativity, are characterized by their remarkable simplicity encapsulated by the no-hair theorem, according to which astrophysical black holes are fully described by only three external parameters: mass, electric charge, and angular momentum [1, 2]. Nevertheless, in extended theories of gravity motivated by string theory, higher-dimensional scenarios, and scalar–tensor frameworks, additional dynamical fields may couple nontrivially to gravity, giving rise to so-called secondary black hole hair and leading to deviations from the standard Schwarzschild and Kerr geometries [3, 4]. Such deviations can, in principle, leave observable imprints in the strong-field regime.

Among these extensions, the Kalb–Ramond field—an antisymmetric rank-two tensor field arising naturally in the low-energy effective action of string theory—plays a prominent role [5–7]. The presence of the Kalb–Ramond field modifies the gravitational sector and can induce effective electromagnetic-like contributions to the spacetime geometry, thereby altering the dynamics of matter fields in the vicinity of compact objects [8]. In spherically symmetric configurations, this framework admits magnetized black hole solutions that retain the Schwarzschild form of the metric at the level of the line element while incorporating an intrinsic magnetic-like parameter associated with the Kalb–Ramond field strength [9, 10]. Such magnetized Schwarzschild black holes provide a theoretically consistent and phenomenologically rich arena for probing strong-field gravity beyond general relativity.

The astrophysical relevance of magnetized black holes has been emphasized in numerous studies, as magnetic fields are expected to be ubiquitous in realistic environments surrounding compact objects, particularly in accretion disks and relativistic jets [11]. These magnetic effects can significantly influence high-energy emission processes in X-ray binaries and active galactic nuclei, motivating detailed investigations of particle dynamics in magnetized spacetimes.

The motion of test particles around black holes constitutes a powerful probe of the underlying spacetime geometry. In particular, the dynamics of electrically charged particles is governed by the interplay between gravitational attraction and Lorentz forces induced by the ambient magnetic field, leading to modified effective potentials, shifts in the locations of circular orbits and

* kmukhabbat98@gmail.com
† Corresponding author: n.kurbonov@newuu.uz

the innermost stable circular orbit (ISCO), as well as altered stability properties of bound trajectories [12–14]. Previous studies have extensively analyzed capture cross-sections and trajectories of massless and massive particles around parameterized and magnetized black holes, revealing significant departures from the standard Schwarzschild and Kerr cases in alternative gravity models [15–17].

Complementary analyses of orbital and epicyclic frequencies in stationary and axially symmetric spacetimes have further elucidated the oscillatory properties of particle motion, which are of direct relevance for modeling quasiperiodic oscillations observed in accreting black hole systems [18–21]. These studies underscore the potential of charged particle dynamics as a diagnostic tool for exploring both the magnetic environment and possible deviations from general relativity in the vicinity of black holes.

II. KALB-RAMOND BLACK HOLES

The spacetime of the KR BH is described in the spherical coordinates $x^\alpha = \{t, r, \theta, \phi\}$ by the line element

$$ds^2 = -f(r)dt^2 + \frac{1}{f(r)}dr^2 + r^2 d\Omega^2, \tag{1}$$

where the lapse function $f(r) = 1/(1-l) - 2M/r$ and $d\Omega^2 = d\theta^2 + \sin^2\theta d\phi^2$. The spacetime turns to the Schwarzschild black hole one when $l = 0$.

III. MAGNETIZATION OF KR SPACETIME

This work assumes that the KR BH is immersed in a uniform external magnetic field. Obtaining analytical solutions to Maxwell's equations for magnetic fields around black holes is more complicated. Wald has performed a simple approach for flat spherically symmetric Ricci spacetime using an analogous uniform electromagnetic field 4-vector A_ϕ and an axial Killing vector ψ_α. To find the Maxwell equation in curved spacetime, one has to use $\frac{1}{\sqrt{-g}}\partial_\alpha(\sqrt{-g}F^{\alpha\beta}) = 0$, where $F_{\alpha\beta} = \partial_\alpha A_\beta - \partial_\beta A_\alpha$; we search for a solution in the form

$$A_\phi = \frac{1}{2}Br^2\psi(r)\sin^2\theta, \tag{2}$$

where $\psi(r)$ is an arbitrary radial (correction) function corresponding to the values of l and for the Schwarzschild limit $l = 0$ the function takes $\psi(r) = 1$. One may get an ordinary differential equation for $\psi(r)$ with l by inserting Eq.(2) into Maxwell's equation

$$\left[\frac{1}{1-l} - \frac{2M}{r}\right] r^2\psi''(r) + 2M\psi'(r) - 2\psi(r) = 0.$$

Eq.(3) is a complicated second-order differential equation to solve analytically. Therefore, we solve it numerically and analyze the $\psi(r)$ function for the various values of l.

$$\psi(r) = \frac{1}{2(l-1)^2} \, {}_2F_1\left(\frac{3}{2} - \frac{1}{2}\sqrt{9-8l}, \frac{1}{2}\sqrt{9-8l} + \frac{3}{2}; 3; \frac{r}{2M(1-l)}\right) \tag{3}$$

One may immediately find the non-zero components of the electromagnetic tensor using the definition $F_{\mu\nu} = A_{\nu,\mu} - A_{\mu,\nu}$ for each configuration of the external magnetic field in the following form,

$$F_{r\phi} = \frac{1}{2}B_0 r\left[r\psi'(r) + 2\psi(r)\right]\sin^2\theta\,, \tag{4}$$

$$F_{\theta\phi} = B_0 r^2\psi(r)\sin\theta\cos\theta\,. \tag{5}$$

Copyright © 2025

The component of the magnetic field around the black hole measured by a local observer read

$$B^{\hat{\alpha}} = \frac{1}{2}\sqrt{g_{\alpha\alpha}}\eta^{\alpha\beta\sigma\mu}F_{\beta\sigma}w_{\mu} , \tag{6}$$

where w_μ is four-velocity of the local static observer, $\eta_{\alpha\beta\sigma\gamma}$ is the pseudo-tensorial form of the Levi-Civita symbol $\epsilon_{\alpha\beta\sigma\gamma}$ with the relations

$$\eta_{\alpha\beta\sigma\gamma} = \sqrt{-g}\epsilon_{\alpha\beta\sigma\gamma} , \qquad \eta^{\alpha\beta\sigma\gamma} = -\frac{1}{\sqrt{-g}}\epsilon^{\alpha\beta\sigma\gamma} , \tag{7}$$

and $g = \det|\mathrm{g}_{\mu\nu}| = -r^4\sin^2\theta$ for spacetime metric (1); $\epsilon_{0123} = 1$ with even permutations and -1 for odd ones, and it is zero for other combinations. The non-zero components take the form

$$B^{\hat{r}} = B_0\psi(r)\cos\theta , \tag{8}$$

$$B^{\hat{\theta}} = \frac{1}{2}B_0\sqrt{f(r)}\,[r\psi'(r) + 2\psi(r)]\sin\theta . \tag{9}$$

IV. ELECTRICALLY CHARGED PARTICLE'S MOTION AND ITS CIRCULAR ORBITS

Here, we investigate the dynamics of electrically charged particles around KR black holes and wormholes immersed in the uniform magnetic field, with a focus on orbits in the and related epicyclic oscillations. The action of electrically charged particles at the equatorial plane (where $\theta = \pi/2$ and $\dot{\theta} = 0$) can be expressed in the form

$$\mathcal{S} = -Et + L\phi + \mathcal{S}_r , \tag{10}$$

which allows the separation of variables in the Hamilton-Jacobi equation. The equation of radial motion of charged particles can be found as

$$\dot{r}^2 = \mathcal{E}^2 - V_{\rm eff}(r) , \tag{11}$$

where $\mathcal{E} = E/m$ is the specific energy of the particles and the effective potential for the radial motion of charged particles has the form:

$$V_{\rm eff}(r,\theta) = f(r)\left[1 + \left(\frac{\mathcal{L}}{r\sin\theta} - \omega_B\psi(r)\sin\theta\right)^2\right] , \tag{12}$$

where $\mathcal{L} = L/m$ is specific angular momentum of the particle.

The figure 1 presents the effective potential $V_{\rm eff}$ for electrically charged particles moving around a magnetized Schwarzschild BH in the framework of KR gravity, plotted as a function of the radial coordinate r/M. The effects of the KR parameter l and the magnetic field coupling parameter ω_B are analyzed through three panels. The left panel illustrates effective potential for a fixed magnetic field parameter ω_B and different values of the KR parameter l. The black solid curve corresponds to the Schwarzschild BH, while other curves represent KR BHs with positive and negative values of l, respectively. Positive values of l increase the height of the effective potential barrier, leading to stronger confinement and enhanced orbital stability. In contrast, negative values of l reduce the potential barrier, weakening the stability of circular orbits. In the middle panel, the Kalb–Ramond parameter l is fixed, while the magnetic field coupling parameter ω_B is varied. The effective potential reaches its maximum value for negative ω_B, while positive values of ω_B lower the potential barrier relative to the Schwarzschild case. This behavior reflects the directional nature of the Lorentz force: a negative magnetic coupling enhances the effective repulsive contribution to the potential, thereby increasing the height of the barrier and stabilizing circular motion, whereas a positive coupling reduces this effect. The right panel shows effective potential for a fixed negative Kalb–Ramond parameter l with different values of the magnetic field coupling ω_B. Similar to the middle panel, negative values of ω_B lead to a higher effective potential barrier compared to positive values. However, due to the negative KR parameter, the overall potential remains lower than in the positive case, indicating reduced orbital stability. Overall, the figure demonstrates that the sign of the magnetic field coupling parameter ω_B plays a crucial role in determining the height and structure of the effective potential.

Circular orbits are performed when $dV_{\rm eff}/dr = 0$. Then one may obtain a relation for the angular momentum of a charged particle at a circular orbit at the equatorial plane ($\theta = \pi/2$)

$$\mathcal{L}_{\pm} = \frac{r\omega_B\big(f(r)\psi(r) - rf(r)\psi'(r) - rf'(r)\psi(r)\big)}{\big(2f(r) - rf'(r)\big)} \pm \frac{r\sqrt{2rf(r)f'(r) - r^2[f'(r)]^2 + \omega_B^2[f(r)]^2[\psi(r) + r\psi'(r)]^2}}{\big(2f(r) - rf'(r)\big)} \tag{13}$$

Copyright © 2025

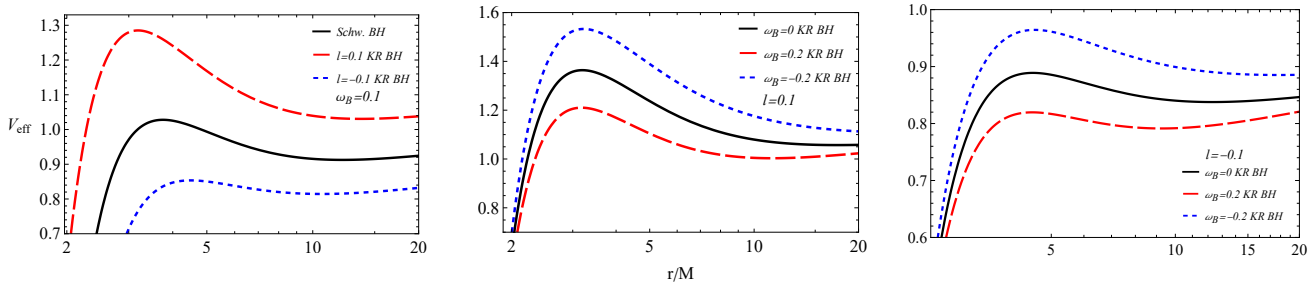


FIG. 1: Radial dependence of effective potencial V_{eff} for electrically charged particles orbiting a magnetized Schwarzschild BH in the framework of KR gravity.

Figure 2 shows the effect of the KR parameter l on the angular momentum $\mathcal{L}$ and energy $\mathcal{E}$ of electrically charged particles moving on circular orbits around a magnetized Schwarzschild BH, for a fixed magnetic field coupling ω_B. On left panel, the angular momentum $\mathcal{L}$ is plotted as a function of the energy $\mathcal{E}$ for circular orbits. It is clearly seen that negative values of the KR parameter lead to higher angular momentum at lower energies, while increasing l shifts the curves toward lower angular momentum and higher energy. This behavior indicates that negative KR corrections strengthen the effective gravitational binding, allowing particles to maintain circular motion with larger angular momentum and reduced energy. On right panel, the energy $\mathcal{E}$ is shown as a function of the radial coordinate r. For all values of l, the energy profile exhibits a minimum corresponding to stable circular orbits. Negative values of l lower the minimum energy and shift it toward smaller radii, indicating that stable orbits can exist closer to BH. In contrast, positive KR parameters raise the energy minimum and push stable orbits outward, reflecting a weakening of the effective binding. Overall, the figure demonstrates that negative KR corrections enhance orbital stability by simultaneously increasing angular momentum and lowering energy, whereas positive corrections act in the opposite direction.

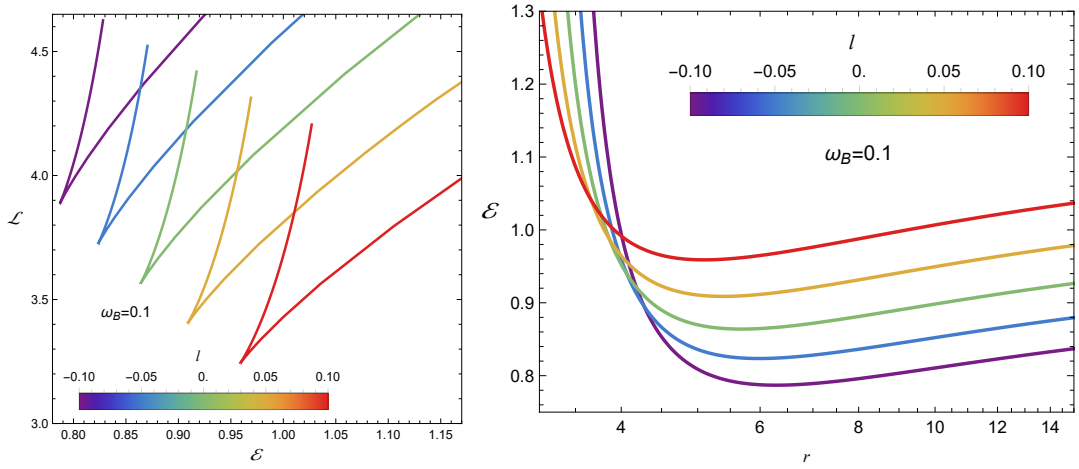


FIG. 2: Dependence of the KR parameter l on the angular momentum $\mathcal{L}$ and energy $\mathcal{E}$ of electrically charged particles.

A. Innermost Stable Circular Orbit of charged particles

In this subsection, we will investigate the ISCO of a charged particle in the vicinity of selected charged black holes [22, 23]. As is well known, the following conditions are currently established for the stability of circular orbits:

$$V_{\text{eff}} = \mathcal{E}, \quad \partial_r V_{\text{eff}} = 0, \quad \partial_{rr} V_{\text{eff}} = 0, \tag{14}$$

where ∂_{rr} denotes the second derivative with respect to r. The first derivative condition identifies stationary points, while the last condition corresponds to a minimum of the effective potential.

Figure 3 illustrates the dependence of ISCO parameters on the magnetic field coupling ω_B and the Kalb–Ramond parameter l for electrically charged particles orbiting a magnetized Schwarzschild BH. In the top left panel, the ISCO radius R_{ISCO} is plotted

Copyright © 2025

as a function of the magnetic field parameter ω_B for different values of l. It is evident that R_{ISCO} decreases monotonically with increasing ω_B for all considered values of the KR parameter. For a fixed magnetic field strength, negative values of l yield larger ISCO radii, while positive values of l shift the ISCO inward. The top middle panel displays the dependence of the ISCO angular momentum $\mathcal{L}_{ISCO}$ on ω_B. For all values of l, the angular momentum increases monotonically as the magnetic field strength grows. At a fixed value of ω_B, the angular momentum is higher for negative KR parameters and lower for positive ones, reflecting the role of the KR field in modifying the balance between gravitational attraction and centrifugal effects. In the top right panel, the ISCO energy $\mathcal{E}_{ISCO}$ is shown as a function of ω_B. The energy decreases monotonically with increasing magnetic field strength for all values of l. Furthermore, for a given magnetic field, negative values of the KR parameter lead to lower ISCO energies, whereas positive values increase the energy. This behavior implies that negative KR corrections enhance the binding energy of circular orbits, while positive corrections weaken it.

The bottom left panel presents the relation between the ISCO angular momentum and the ISCO radius for different values of the KR parameter. In this case, $\mathcal{L}_{ISCO}$ decreases as R_{ISCO} increases. For a fixed radius, negative values of l correspond to higher angular momentum, while positive values yield lower angular momentum, demonstrating that the KR field significantly modifies the angular momentum–radius relation at the ISCO.

Finally, the bottom right panel shows $\mathcal{L}_{ISCO}$ as a function of R_{ISCO} for different magnetic field strengths. In contrast to the previous panel, the angular momentum increases with increasing ISCO radius. For a given radius, positive magnetic coupling produces larger angular momentum values, while negative magnetic coupling yields smaller ones, highlighting the directional dependence of the Lorentz force acting on the charged particles.

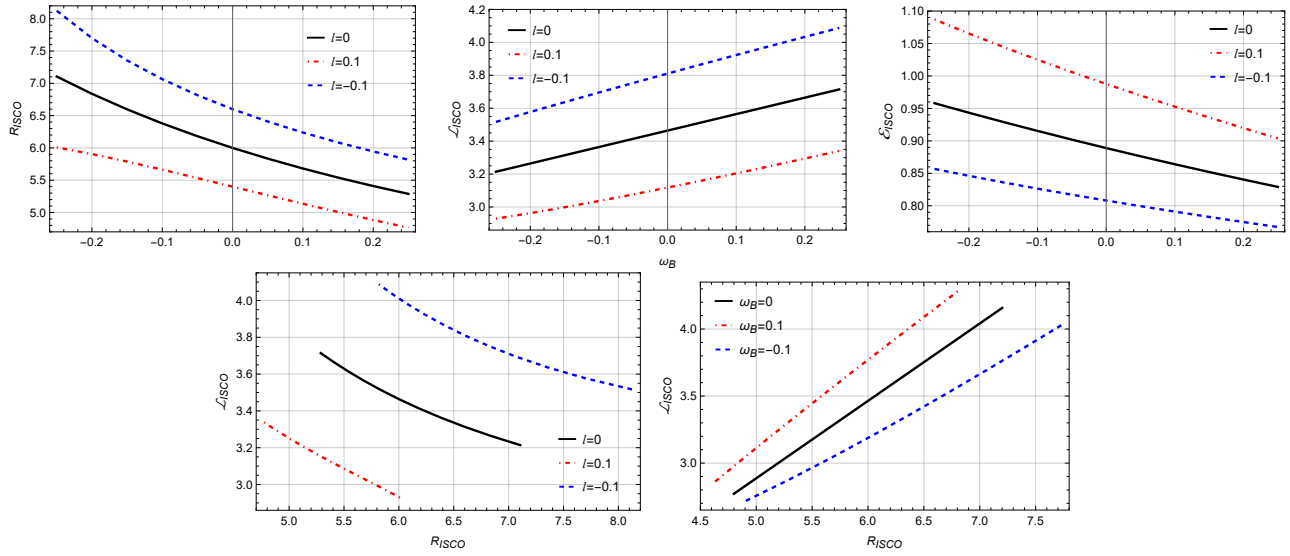


FIG. 3: The dependence of the ISCO radius R_{ISCO}, angular momentum $\mathcal{L}_{ISCO}$, and energy $\mathcal{E}_{ISCO}$ on the magnetic field coupling parameter ω_B and the Kalb–Ramond parameter l.

V. CONCLUSION

In this work, we have investigated the dynamics of electrically charged particles orbiting magnetized Schwarzschild BHs within the framework of KR gravity. By incorporating both an external uniform magnetic field and the KR parameter into the spacetime geometry, we analyzed how deviations from standard general relativity influence effective potentials, circular orbits, and the properties of the ISCO. Our analysis of the effective potential demonstrates that both the magnitude and the sign of the magnetic field coupling parameter play a crucial role in determining orbital stability. Negative magnetic coupling enhances the effective potential barrier and stabilizes circular motion, whereas positive coupling weakens confinement. The KR parameter further modifies this behavior: positive values increase the effective potential barrier and strengthen confinement, while negative values reduce the barrier height and weaken orbital stability. These results highlight the nontrivial interplay between gravitational, electromagnetic, and KR field effects in charged particle dynamics. We have shown that the energy and angular momentum of circular orbits are strongly affected by the KR parameter. In particular, negative values of the KR parameter allow circular orbits with higher angular momentum at lower energies, indicating enhanced gravitational binding. Conversely, positive KR corrections raise the orbital energy and reduce angular momentum, reflecting a weakening of the effective binding. The ISCO analysis reveals that increasing the magnetic field strength shifts the ISCO radius inward, increases the required angular

Copyright © 2025

momentum, and lowers the ISCO energy for all considered values of the KR parameter. At fixed magnetic field strength, negative KR corrections shift the ISCO outward, increase angular momentum, and decrease energy, while positive corrections produce the opposite effect. These results demonstrate that the KR field leaves a clear imprint on the stability boundary of circular motion around magnetized BHs. Overall, our findings show that the combined influence of external magnetic fields and KRd gravity leads to significant modifications in the orbital structure of charged particles around Schwarzschild BHs. Such effects may have important implications for astrophysical processes in magnetized accretion environments and could provide potential observational signatures of string-inspired gravity corrections. Future work may extend this analysis to rotating BHs, include plasma effects, or explore observable consequences for quasi-periodic oscillations and high-energy emissions.

REFERENCES

[1] S. W. Hawking, Commun. Math. Phys. **25**, 152 (1972).
[2] J. D. Bekenstein, (1998), arXiv:gr-qc/9808028 [gr-qc].
[3] T. P. Sotiriou and V. Faraoni, Phys. Rev. Lett. **108**, 081103 (2012).
[4] P. Pani and V. Cardoso, Phys. Rev. D **79**, 084031 (2009).
[5] M. Kalb and P. Ramond, Phys. Rev. D **9**, 2273 (1974).
[6] G. T. Horowitz and A. Strominger, Nucl. Phys. B **360**, 197 (1991).
[7] A. Sen, Phys. Rev. Lett. **69**, 1006 (1992).
[8] S. Kar, S. Lahiri, and S. SenGupta, Phys. Lett. B **750**, 319 (2015).
[9] A. N. Aliev and D. V. Gal'tsov, Sov. Phys. Usp. **32**, 75 (1989).
[10] R. M. Wald, Phys. Rev. D **10**, 1680 (1974).
[11] M. A. Abramowicz and P. C. Fragile, Living Rev. Relativity **16**, 1 (2013).
[12] A. N. Aliev and N. Özdemir, Mon. Not. R. Astron. Soc. **336**, 241 (2002).
[13] J. Rayimbaev, B. Narzilloev, A. Abdujabbarov, and B. Ahmedov, Galaxies **9**, 71 (2021).
[14] O. Z. Stuchlík and J. Kovař, Int. J. Mod. Phys. D **17**, 2089 (2008).
[15] B. Toshmatov, O. Rahimov, B. Ahmedov, and A. Ahmedov, Galaxies **9**, 65 (2021).
[16] B. Ahmedov, O. Rahimov, and B. Toshmatov, Universe **7**, 307 (2021).
[17] O. Rahimov, B. Toshmatov, Y. Vyblyi, A. Akhmedov, and B. Abdulazizov, Physics of the Dark Universe **44**, 101483 (2024).
[18] M. A. Abramowicz and W. Kluźniak, Astron. Astrophys. **374**, L19 (2001).
[19] B. Turimov and O. Rahimov, Universe **8**, 507 (2022).
[20] B. Turimov, O. Rahimov, B. Ahmedov, Z. Stuchlík, and K. Boymurodova, International Journal of Modern Physics D **30**, 2150037-407 (2021).
[21] B. Turimov, A. Mamadjanov, and O. Rahimov, Galaxies **11**, 70 (2023).
[22] J. Rayimbaev, N. Kurbonov, A. Abdujabbarov, and W.-B. Han, Int. J. Mod. Phys. D **31**, 2250032 (2022).
[23] A. Demyanova, O. Rakhimov, Y. Turaev, N. Kurbonov, and J. Rayimbaev, in *RAGtime 20-22: Workshops on Black Holes and Neutron Stars*, edited by Z. Stuchlík, G. Török, and V. Karas (2020) pp. 19–27, proceedings of RAGtime 20-22.

 Copyright © 2025